Article

Discovery of Novel Turn-On Fluorescent Probes for Detecting PDE# Protein in Living Cells and Tumor Slices

Gaopan Dong, Long Chen, Jing Zhang, Tingting Liu, Lupei Du, Chunquan Sheng, and Minyong Li

Anal. Chem., **Just Accepted Manuscript** • DOI: 10.1021/acs.analchem.0c00335 • Publication Date (Web): 22 Jun 2020

Discovery of Novel Turn-On Fluorescent Probes for Detecting PDEδ Protein in Living Cells and Tumor Slices

Gaopan Dong [a,†], Long Chen [b,†], Jing Zhang [c,†], Tingting Liu [a,d], Lupei Du [a], Chunquan Sheng [b,*] and Minyong Li [a,*]

[a] Department of Medicinal Chemistry, Key Laboratory of Chemical Biology (MOE), School of Pharmaceutical Sciences, Cheeloo College of Medicine, Shandong University, Jinan, Shandong 250012, China.

[b] Department of Medicinal Chemistry, School of Pharmacy, Second Military Medical University, Shanghai 200433, China.

[c] Department of Pathology, Changhai Hospital, Second Military Medical University, Shanghai 200433, China.

[d] Institute of Pharmacology, School of Pharmaceutical Sciences, Shandong First Medical University & Shandong Academy of Medical Sciences, Taian 271000, Shandong, China.

†Authors contributed equally to this work.

* Corresponding Author: Tel/Fax: +86-531-8838-2076. Email: mli@sdu.edu.cn; shengcq@smmu.edu.cn.

ABSTRACT: The first small molecule fluorescent turn-on probes for detecting PDEδ protein were rationally designed, which showed reasonable fluorescent properties and can be applied into visualizing the PDEδ protein at the living cell and tissue levels. The qPCR results showed that the mRNA expression of *KRAS*, *PDEδ*, *AKT1*, *MAPK1*, *MEK7*, *RAF1* and *mTOR* were down-regulated by probes **1-3** through PI3K/AKT/mTOR and MAPK signal pathways. The probes also can down-regulate the protein level of pErk and tErk. Therefore, these small-molecule fluorescent probes are expected to be used into screening anti-pancreatic cancer drugs targeting on the PDEδ protein, as well as in better understanding the pathological and physiological roles of PDEδ protein.

INTRODUCTION

Pancreatic cancer is considered as the fourth lethal cancer in the United States, and is highly possible raised to the 2nd place by the year 2030.[1,2] Pancreatic cancer as a fatal disease and one of the most leading cause of cancer-related deaths among all malignances, for it with a horrible mortality rate and the 5-year survival rate of pancreatic cancer less than 5%.[1-5] It's reported that during 2006 to 2010, the pancreatic cancer incidence rate had increased by 1.3% per year.[3] Hence, there is an unquestionably need to find effective systemic therapies to overcome this highly lethal cancer.

The oncogenic *KRAS* gene was first associated with pancreatic cancer more than thirty years.[2,6] Under physiological conditions, the *KRAS* gene plays a crucial role in regulating cell growth, while under abnormal conditions, the mutant *KRAS* gene can lead to sustained cell growth, finally drive pancreatic neoplasia.[5,7] The RAS proteins family include KRAS, NRAS and HRAS, and Ras proteins are present with binary on-off switches: the GTP-bound form is ON, or else the GDP-bound form is OFF,[5,8] so the Ras proteins play a crucial role in cytoplasmic signal transmission and participate in regulating diverse normal cellular functions.[9] The mutant KRAS protein is highly prevalence in pancreatic (>90%), colorectal (about 50%), and lung (30%) cancers.[5,7,8,10-13] KRAS protein played a direct causal role in human cancer neoplastic,[8] oncogenic *KRAS* could induce metabolic disorders, while the aberrant metabolism is considered as a primary cause leading to cancer. [5,14,15] Thus, intensive efforts were carried on the KRAS protein research; the researchers take the oncogenic KRAS as a prime therapeutic target for pancreatic cancer. However, Ras proteins have not yielded to any types of therapeutics, which was regarded as "undruggable" for many years, even was compared to "the Everest" to climb.[5,9]

Phosphodiesterase 6 (PDE6) delta subunit (PDEδ), also known as PDE6D, is the δ subunit of rod specific cyclic GMP phosphodiesterase.[7] PDEδ binds and solubilizes the farnesylated Ras proteins, and then facilitate the KRAS protein diffusion in the cytoplasm.[16-19] Bastiaens's group [16] reported that the activity of PDEδ is mediated by the Ras-dependent signaling, and then affect the Ras protein dynamic distribution in the cell. So many researchers turn to take the PDEδ as a therapeutic target for pancreatic cancer.

Nowdays, there are two main pathways to therapeutic target on the oncogenic *KRAS*: small interfering RNA (siRNA) [9,10,13] mediated drug-sensitization on the

oncogenic *KRAS* gene, and novel small-molecule inhibitors disturping KRAS-PDEδ interactions.[9] siRNA only down-regulate gene expression, while the small-molecule inhibitors showed great advantages in regulating the functions of gene.[9] Based on an extensive biochemical study, small molecule inhibitors could inhibit the KRAS-PDEδ interactions, and impair the oncogenic KRAS signaling was reported.[18,20] Zimmermann et al. found deltarasin could block RAS signaling, reduce the proliferation of pancreatic cancer cell, and even lead to cancer cell death.[18] However, there are also many disadvantages for deltarasin, such as poor selectivity and significant cytotoxicity. Subsequently, a new PDEδ inhibitor, named deltazinone was reported to be highly selective, and less cytotoxic than deltarasin. It was demonstrated to have a high correlation with the phenotypic effect of PDEδ.[19] Even though, the therapeutic effects of these KRAS-PDEδ inhibitors on pancreatic cancer were far from clinical application. Previously, our group used fragment-based drug design (FBDD) to discover and design novel chemotypes of KRAS–PDEδ inhibitors, targeting on the Arg61 pocket and the Tyr149 pocket. Biochemical evaluations demonstrated our novel PDEδ inhibitors were druggable and effective on the inhibition of the KRAS-PDEδ protein-protein interactions (PPI).[7]

Recently, small-molecule fluorescent probes are prevalently used into imaging and detecting biotargets. Compared with traditional methods such as bimolecular fluorescence complementation (BiFC) assay or autofluorescent translocation biosensor techniques, small meculor fluorescent probes have the advantages of convenient and affordable detection. Most importantly, they possess turn-on switch mechanism, which are highly efficient and sensitive in imaging and detecting target proteins[21-24] even in the high signal-to-background ratios environment.[25,26] Inspired by our previous work,[7] we envisioned that novel turn-on small-molecule fluorescent probes for PDEδ protein could be designed by incoporating environmental sensitive fluorophores on PDEδ inhibitors. Herein the first fluorescent probes for PDEδ were identified on the basis of the binding mode of quinazolinone inhibitors, which were able to selectively in detecting and imaging PDEδ in the pancreatic cancer cell lines and tumor slices. They are valuable chemical tools for better understanding the pathological and physiological functions of PDEδ protein and development of new drug screening assay.

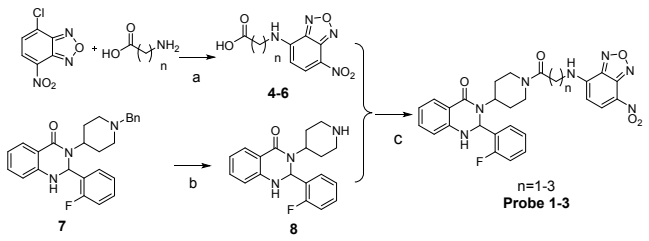

Scheme 1. Synthetic routes of fluorescent probes **1-3**. a) $NaHCO_3$, MeOH, r.t., 24 h, 62%-77%; b) H_2, $Pd(OH)_2$, MeOH, r.t., overnight, 85% ; c) HBTU, TEA, DMF, r.t., 2 h, 16%-53%.

EXPERIMENTAL SECTION

Materials and Instruments. The chemicals related to synthesis probes were purchased from commercial sources. NMR were assayed by the Bruker NMR spectrometer. Photophysical properties were assayed by the Shimadzu UV-2401PC UV-visible spectrometer and Bio Tek microplate reader. The cell images were captured by the Zeiss Axio Observer A1 fluorescence microscope. The purity of probes were analyzed by Agilent Technologies 1260 Series HPLC with a C18 reversed phase column (250 x 4.60mm , Phenomenex). The Immunohistochemical and tumor slice images were captured by OLYMPUS VS120 microscope, Beckman CytoFLEX flow cytometry was used for assay the binding ability of probes to living cell, the qPCR were assayed by LightCycler® 96 SW 1.1 qPCR instrument (Roche, Switzerland).

Synthesis. The synthetic route for preparation of probes **1-3** was shown in **Scheme 1**. NBD-Cl reacted with different amino acid to produce compounds **4-6**. Subsequently, the reaction of intermediates **4-6** with compound **8**, HBTU, and TEA was conduct to afford the fluorescent probes **1-3**. Synthetic protocols and structure characteriztion can be found in the **Supporting Information**.

Spectroscopy Assay of Probes 1-3. The Fluorescence spectra of probes **1-3** are assayed at 5 μM and diluted into 1×PBS buffer and then scaned by UV-visible spectrometer, BioTek microplate reader and HitachiF-2500 fluorescent spectrometer. Further informations of the photophysical properties of probes **1-3** are provided in **Supporting Information**.

Fluorescence Anisotropy Assay. The fluorescence anisotropy assay was referenced to our previous report.[7,27] Determination of equilibrium dissociation constants K_{D2} for each compound was performed using the fluorescence anisotropy assay with Atrovastatin-PEG3-FITC as ligand in 96-well flat-bottom black plates (Corning # 3650), further information can be found in **Supporting Information**.

***In Vitro* Anti-proliferative Assay.** We assay the cytotoxicity of probes **1-3** and deltazinone in pancreatic cell lines by the CCK-8 method. We selected two pancreatic cell lines Capan-1 and MIA PaCa-2 to test the cytotoxicity of probes **1-3**. 5×10^3 cells each well were planted into the 96-wells transparent plate and added 100 μL Dulbecco's Modified Eagle Medium (DMEM) high glucose complete medium with 1% Penicillin-Streptomycin, 10% FBS and MIA PaCa-2 cell line also needed 5% house serum, then the 96-well plates were cultured in 37 ℃ with 5% CO_2 humidified atmosphere for 12h. Then probes **1-3**/deltazinone were added to the wells with a series of concentrations (3.125, 6.25, 12.5, 25, 50 and 100 μM), respectively. Cells in the 96-well plates were treated with probes **1-3** or deltazinone for another 48 h. Finally, followed the manufacturer instruction of CCK-8 kit, all the

absorbance values at 450 nm of each well were recorded by BMG multiscan spectrum. All the absorbance values were analyzed by GraphPad Prism 7.0 software and got the IC_{50} value of each probe. Furture informations are provided in **supporting informations**.

Fluorescence Imaging in Living Cells. MIA PaCa-2 and Capan-1 cells are selected for the cell imaging assay. Cells were transferred into confocal dish at the proliferation period, and cultured for 12 h. Then, probes **1-3** were diluted into DMEM medium (without FBS) and got a 5 μM probe solution, all cells were co-staining with the nuclear dye (500 nM Hoechst 33342). All the cells were cultured at 37 ˚C atmosphere for 15 min, respectively. We also set MIA PaCa-2 cell line and Capan-1 cell line co-incubated with KRAS-PDEδ inhibitor deltazinone (100 μM) and 5 μM probe as the positive control group. At the same time, we also chosen the normal cell line HEK-293 cells at the negative control incubated with 5μM probe. All the fluorescence imagings in living cell lines were captured by the Zeiss Axio Observer A1 fluorescent microscope. The background of each image was adjusted by Image J software. Objective lens: 63×.

Flow Cytometry Analysis the Binding Ability of Probes 1-3 to Living Cell Lines. The flow cytometry test was performed on MIA PaCa-2 and Capan-1 cell lines. MIA PaCa-2 and Capan-1 cells were collected and washed by PBS for thrice. 5 μM probe was added together with deltazinone (100 μM) or solely incubated with 1×10^5 cells in 300 μL PBS (pH=7.4), respectively, then all the cells were added into the flow tubes. After incubation for about 0.5 h at 37 ˚C in the dark environment, the fluorescence intensity of cells were assayed by Beckman CytoFLEX Cell Counter.

The Total RNA Isolation, cDNA Synthesized and qPCR Test the Relative Expression Level of Related mRNA. When the MIA PaCa-2 at the proliferation period, the cells were collected and planted into the 6 well paltes. Total RNA was extracted from MIA PaCa-2 cell and Capan-1, using RNAiso Plus reagent (TaKaRa, Dalian, China). 1.5 μg total RNA was reversed transcription to cDNA with HiFiscript cDNA synthesis kit (CWBIO, CW2569M, Beijing, China), following the manufacturer's instructions. The cDNA were stored at −20˚C until use. Quantitative real-time PCR was performed by the FastStart Universal SYBR Green Master (ROX) (Roche, Switzerland), and then performed by the LightCycler® 96 SW 1.1 qPCR instrument (Roche, Switzerland) at a final volume of 10 μL followed the cycle parameters recommended by the manufacturer. Relative expression levels of *KRAS*, *PDEδ*, *AKT1*, *MAPK1*, *MEK7*, *RAF1* and *mTOR* were calculated by the $2^{-\Delta\Delta CT}$ method,[28,29] and GAPDH as the reference gene. The primers of each gene for qPCR are shown in **Table s3**.

Western Blot. Mia PaCa-2 cells were seeded at a density of 5×10^5 each well in 6-well plates. After 24 h incubation, cells were stimulated with 125 ng/ml EGF for 5 min and then treated with various concentrations of compounds for 2 h. Briefly, add appropriate amount of ice-cold lysis buffer containing protease inhibitor (Sigma) and phosphatase inhibitor I and II (Sigma) to each plate well. Scraped off on ice and shake gently for 15 min. Collect the lysate, transfer to a microcentrifuge tube and centrifugate at 4 °C, 12,000g for 15 min. The extracted protein was denatured in boiling water for 5 min. 30 μg protein samples from each lysate were separated by SDS-PAGE, then transferred to the PVDF membranes (Merck Millipore) and then blocked for 2 h in the 5% BSA blocking solution at room temperature. The membranes were incubated with the primary antibody overnight in dark at 4 ˚C. Then probed with the appropriate secondary antibody for 2 h. After washed by TBST for three times, the PVDF membranes were decteted by chemiluminescence (Thermo Scientific Pierce ECL Western Blotting) and scanned by Chemiluminescence imaging system. More informations can be found in the **Supporting Informations**.

Immunohistochemical (IHC) Analysis of Capan-1, HeLa Tumor Slices and Normal Mouse Skin Tissue Slices. The Capan-1 cells and HeLa cells were grafted subcutaneously under the forelimb armpit of BALB/c nude mice, respectively. After 25 days, Capan-1 and HeLa tumors were harvested, and fixed with 10% formalin for 24 h, and then embedded by paraffin. Subsequently, the tumors were sectioned into 3 μm thickness layers. According to the protocol of IHC, after antigen repaired, the slices were incubated with primary anti-KRAS antibody (1:150, Catalog Number: 12063-1-AP, Proteintech) at 4 °C for 12h, then followed the protocol of IHC as we previous reported.[25] Tumor sections were photoed by OLYMPUS VS120 virtual slide microscope, with a 40× objective len.

Fluorescence Imaging Analysis of Capan-1, HeLa Tumor Tissue Slices and Normal Mouse Tissue Sections. 10 mM probes solutions diluted with Krebs buffer (pH=7.4) at 1:1000, and get a final concentration of 10 μM. After antigen repaired, the tissue sections were labeled by probes **1-3** at 4 ˚C for 12h, Capan-1 tumor slice incubated with probe and 200 μM deltazinone was set as the positive group. Then tissue sections were photoed by OLYMPUS VS120 virtual slide microscope, with a 40× objective len.

RESULTS AND DISSCUSION

Design of Novel Small-molecule Fluorescent Probes. Previously, we designed quinazoline inhibitors by structural biology-inspired FBDD.[7] The binding mode of quinazoline inhibitor (**Figure 1A**) with PDEδ revealed that the two quinazoline fragment was located into the Arg61 and Tyr149 pocket, respectively (PDB code: 5X73, **Figure 1B**). Considering the hydrophobic nature of the Tyr149 pocket, the quinazoline group was replaced by the environmentally sensitive fluorophore 4-nitrobenzoxadiazole (NBD). As a result, fluorescent probes **1-3** with various linker length were designed **(Figure 1A)**. Molecular docking studies of **probe 2** indicated that the it bound to the PDEδ hydrophobic pocket and kept the key hydrogen bonding interactions with Arg61 (**Figure 1C**). Furthermore, hydrogen bonding

interactions with Gln78, π-π interaction with Trp32 were observed, while the NBD moiety mainly form the hydrophobic interaction with the Tyr149 pocket.

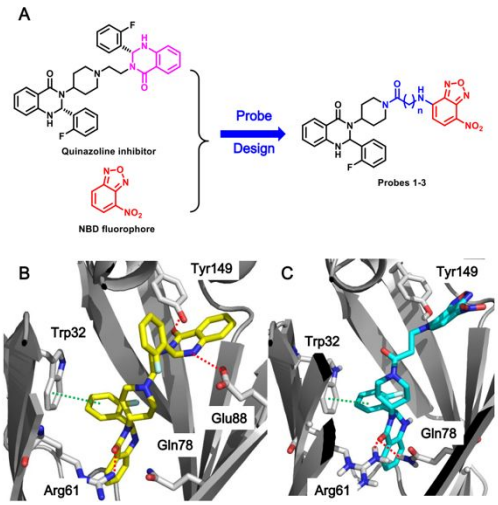

Figure 1. Design of novel small-molecule fluorescent probes of KRAS-PDEδ interaction. (A) Structure-based design of fluorescent probes **1-3** by incorporating NBD fluorophore into the quinazoline inhibitor. (B) Co-crystal structure of quinazoline inhibitor with PDEδ protein (PDB code: 5X74). (C) Proposed binding mode of **Probe 2** with PDEδ protein. Red dash lines represent hydrogen bonding interactions. Green dash lines represent π-π interaction.

Spectroscopic Properties and Turn-On Response to PDEδ Protein of Probes 1-3. The spectroscopic properties of probes **1-3** were measured by the Bio Tek Instruments microplate and the results were showed in **Table 1**. All probes presented excellent fluorescent properties (**Figure S1**). The fluorescence quantum yields of probes **1-3** is 2-5% in the PBS (pH=7.4), while the fluorescence quantum yields of probes **1-3** presented a huge increased in the DMSO solution (27.61-31.42%). These results indicated that probes **1-3** possessed the environment-sensitive turn-on mechanism. We also test whether probes **1-3** own turn-on mechanism to PDEδ protein, from the emission spectrum of probes **1-3** (1 μM) before and after adding PDEδ protein, we found that the fluorescence intensity of probes **1-3** were obviously increased when incubated with PDEδ protein than incubated probes **1-3** or PDEδ protein alone (**Figure 2**). And the fluorescence intensity gradually increased with the increase of PDEδ protein concentration (0-2 μM). The results shown that probes **1-3** own turn-on response to PDEδ protein. Which provide many advantages in the following tests.

Table 1. Fluorescent Properties of Probe 1-3

compd	λ_{max} (nm)	λ_{ex} (nm)	λ_{em} (nm)	Φ(%) PBS	Φ(%) DMSO
Probe 1	337/476	340/470	555	4.99	27.74
Probe 2	342/476	345/475	555	3.21	27.61
Probe 3	342/476	345/480	555	2.46	31.42

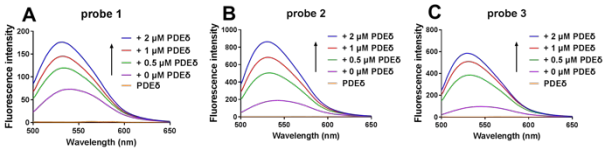

Figure 2. Fluorescence-emission spectra of probes **1-3** (1 μM) before or after added PDEδ protein (0-2 μM). A: probe **1**; B: probe **2**; C: probe **3**.

PDEδ Binding Affinity Assay. The binding affinity to PDEδ of probes **1-3** were presented in **Table 2**, we found that with the fluorophore was introduced to the pharmacophore, the binding affinity of probes to PDEδ were decreased. Among the three novel probes, the K_{D_2} of probes **2-3** is 440 nM and 501 nM, respectively, which is similar to the leading compound (K_{D_2}=465 ± 65 nM).[7]

Cytotoxicity Assay. The cytotoxicity of probes **1-3** and deltazinone were tested in pancreatic cell lines: MIA PaCa-2 and Capan-1 cell by CCK-8 method. From the **Table 2**, we found that our probes can inhibit the tumor cell proliferation, especially the probe **2** and **3** can inhibit the pancreatic tumor cell proliferation better than deltazinone, the IC_{50} values of probe **2** and **3** were 24.71 μM, 15.88 μM in MIA PaCa-2 cell line and 30.89 μM, 33.39 μM in Capan-1 cell line, respectively. These antiproliferative results proved that probes **1-3** may be used as the antitumor drugs.

Table 2. Biological Data of Probes 1-3

compd	K_{D_2} (nM)	IC_{50} (μM)	
		MIA PaCa-2	Capan-1
Probe 1	682 ± 91	37.7±4.18	43.4±8.83
Probe 2	440 ± 73	24.7±4.48	30.9±7.88
Probe 3	501 ± 82	15.9±1.28	33.4±8.25
Deltazinone	1.06 ± 0.55	61.6±4.07	35.3±1.54

Fluorescence Imaging. Based on the excellent fluorescent properties of probes **1-3**, which were used into detecting and imaging PDEδ protein in the living cell lines: KRAS-dependent MIA PaCa-2 cells and Capan-1. The MIA PaCa-2 living cell imaging results indicated that probes **1-3** possess strong fluorescence and could rapidly response to the PDEδ protein in cells, when co-staining with the nuclear dye 500 nM Hoechst 33342, we found that the our probes **1-3** mainly labeled in the plasma membrane, which demonstrated that PDEδ protein was mainly located in the plasma membrane instead of the nuclear (**Figure 3-5**). Furthermore, we also set MIA PaCa-2 and Capan-1 cell lines co-incubated with 5 μM probes **1-3** and 100 μM deltazinone, respectively. The results showed that the fluorescence intensity of probes were decreased by deltazinone, which indicated that deltazinone could competitively binding to PDEδ with our probes. We also chosen the normal HEK

293 cell line, as the negative control, when HEK 293 cells incubated with 5 μM probes **1-3** in the same condition, respectively. The results demonstrated that the fluorescence in HEK 293 cell imagings are weaker than that in the oncogenic KRAS-dependent cell lines, which is in line with our hypothesis. The results provided that our probes **1-3** displayed favorable selectivity for the oncogenic KRAS-dependent cell lines. The Capan-1 cell imaging results were in line with MIA PaCa-2 cell imaging results (**Figures S4-6**).

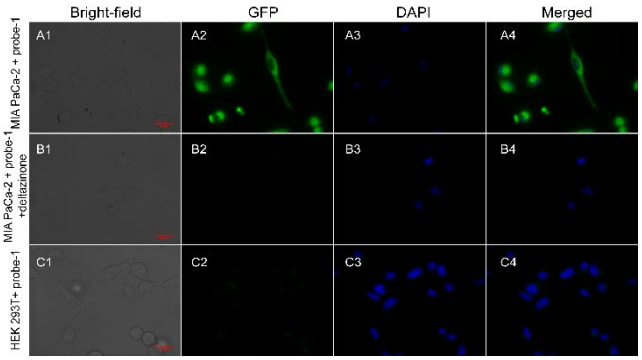

Figure 3. Fluorescence imagings of MIA PaCa-2 and HEK 293 cell lines incubated with probe **1** (5 μM; Bright field: A1-C1; GFP channel: A2-C2; DAPI channel: A3-C3; merged image: A4-C4). A: MIA PaCa-2 cells incubated with 5 μM probe **1**; B: MIA PaCa-2 cells co-incubated with 5 μM probe **1** and 100 μM deltazinone; C: HEK 293 cells incubated with 5 μM probe **1**. Scale bar=67 μm.

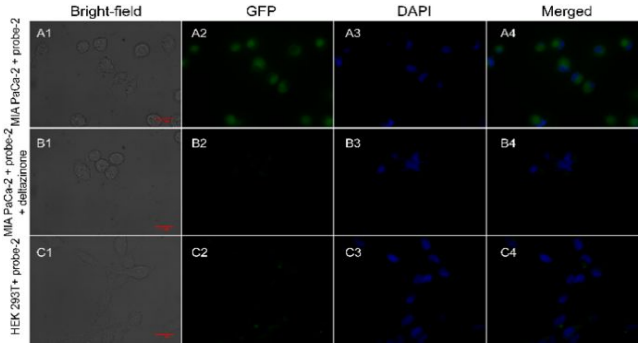

Figure 4. Fluorescence imagings of MIA PaCa-2 and HEK 293 cell lines incubated with probe **2** (5 μM; Bright field: A1-C1; GFP channel: A2-C2; DAPI channel: A3-C3; merged image: A4-C4). A: MIA PaCa-2 cells incubated with 5 μM probe **2**; B: MIA PaCa-2 cells co-incubated with 5 μM probe **2** and 100 μM deltazinone; C: HEK 293 cells incubated with 5 μM probe **2**. Scale bar=67 μm.

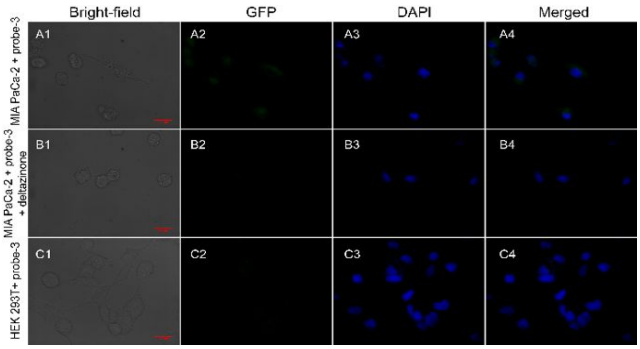

Figure 5. Fluorescence imagings of MIA PaCa-2 and HEK 293 cell lines incubated with probe **3** (5 μM; Bright field: A1-C1; GFP channel: A2-C2; DAPI channel: A3-C3; merged image: A4-C4). A: MIA PaCa-2 cells incubated with 5 μM probe **3**; B: MIA PaCa-2 cells co-incubated with 5 μM probe **3** and 100 μM deltazinone; C: HEK 293 cells incubated with 5 μM probe **3**. Scale bar=67 μm.

Flow Cytometry (FCM) Assay. The binding ability to MIA PaCa-2 living cell line of probes **1-3** were further validated by flow cytometry (FCM). The FCM results exhibited the fluorescence intensity of MIA PaCa-2 incubated with 5 μM probes were stronger than of MIA PaCa-2 co-incubated with 5 μM probes and 100 μM deltazinone, which indicated that the binding capability of our probes **1-3** to the MIA PaCa-2 cells was much higher than to MIA PaCa-2 cells co-incubated with 5 μM probes and 100 μM deltazinone (**Figure 6**), which is in line with the fluorescence microscopic imaging results in MIA PaCa-2 cells. And the FCM results of Capan-1 cell line were disclosed in **Figure S7**. Further details can be found in the **Supporting Information**.

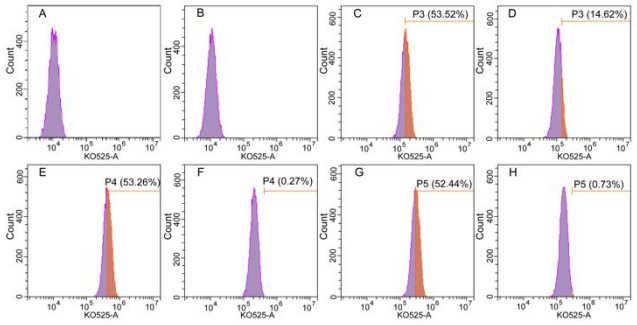

Figure 6. Flow cytometry results of 5 μM probes **1-3** and 100 μM deltazinone binding to the living cells of MIA PaCa-2. A: blank; B: 100 μM deltazinone; C: 5 μM probe **1**; D: 5 μM probe **1**+100 μM deltazinone; E: 5 μM probe **2**; F: 5 μM probe **2**+100 μM deltazinone; G: 5 μM probe **3**; H: 5 μM probe **3**+100 μM deltazinone.

Detecting the Relative Expression Level of mRNA by qPCR. To well analyze the oncogenic KRAS-dependent MIA PaCa-2 cells incubated with probes **1-3**, whether can change the transcriptional levels of related genes encoding KRAS and PDEδ after treated by probe **1-3** The qPCR results showed that the MIA PaCa-2 cells incubated with probes **1-3** for 4 hours, the transcriptional levels of *KRAS* and *PDEδ*

were down-regulated significantly compared with the control group (with 0.1% DMSO) (**Figure 7**), the results demonstrate that probes **1-3** could significantly reduce the relative mRNA expression level of *KRAS* and *PDEδ* (**Figure 7**), and probes **1-3** could also mediate MAPK and PI3K/AKT/mTOR signal pathways, and affect the mRNA expression level of *AKT1*, *MAPK1*, *MEK7*, *RAF1* and *mTOR*, from the qPCR results we found these genes were also down-regulated by probes **1-3**, and interfered cell growth, proliferation, differentiation and apoptosis.[7,27,30]

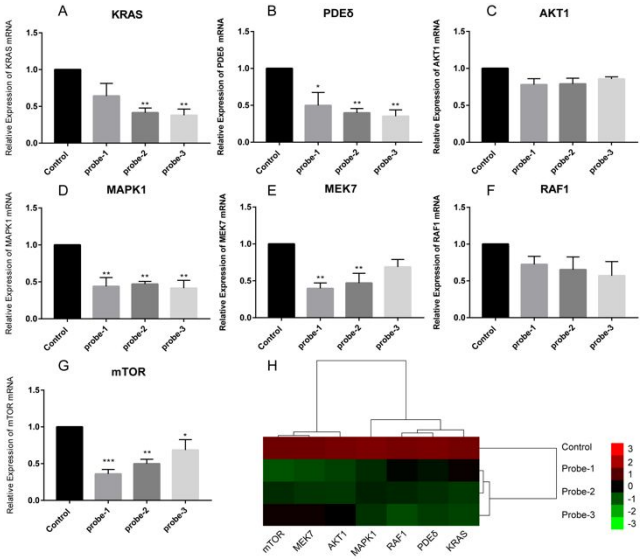

Figure 7. The mRNA expression level dected by qPCR. A: KRAS; B: PDEδ; C: AKT1; D: MAPK1; E: MEK7; F: RAF1; G: mTOR and H: cluster analysis of genes in each groups. All the histograms were present with mean ± SEM, all data were analysed by one-way ANOVA followed by multiple comparisons. The level of significance was defined as $^{*}p<0.05$, $^{**}p<0.01$ and $^{***}p<0.001$ *vs*. control group.

Detecting the Protein Level by Western Blot. We also used the western blot to detect the protein level of PDEδ, tErk, and pErk, pAkt and tAkt in MIA PaCa-2 cell line. As depicted in **Figure 8**, probe **2** could down-regulate the level of tErk, and pErk, which is consistent with the qPCR results, and the ratio of p-Erk/t-Erk showed a dose-dependent manner. Moreover, probe **2** can mediate the MAPK and PI3k/AKT/mTOR signal pathways.

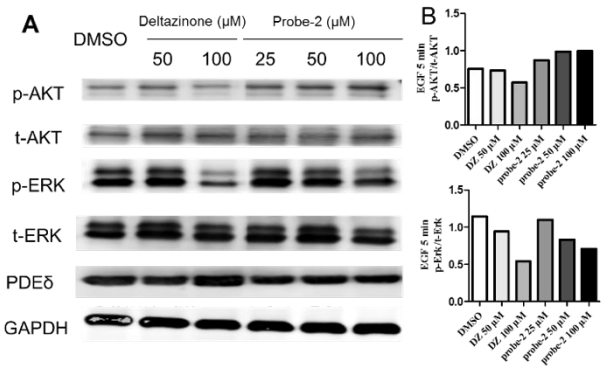

Figure 8. The protein expression level treated with probe **2** and detecting by Western Blot (MIA PaCa-2 cells). A: the band images of protein; B: the quantitative results of protein by the gray values of band from **A** with Image J software, respectively.

Hematoxylin-Eosin Staining(HE) and IHC Assay. The HE staining results shown that the Capan-1 and HeLa tumor slices showed high level of diseased. To furture detecting the protein level of KRAS in tissue level, IHC assay was carried out. The IHC relusts showed that the anti-KRAS antibody could selectively label the oncogenic KRAS tumor, Capan-1 tumor slice was staining the highest immunostaining with anti-KRAS antibody (Proteintech, Wuhan, China), while the normal mice skin tissue showed the least staining (**Figure 9**). The results indicated the Capan-1 tumor expression more KRAS protein than HeLa tumor and normal mice skin tissue. The IHC results provided the bases for the tissue slices imaging test.

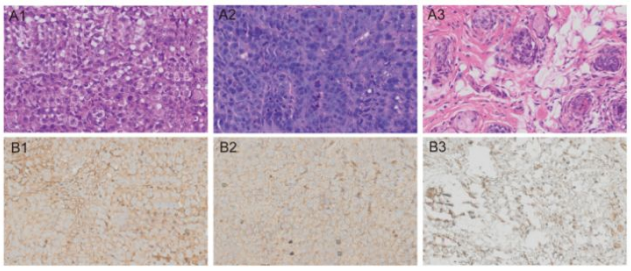

Figure 9. IHC of Capan-1 tumor, HeLa tumor and the normal skin of BALB/c nude mice forelimb armpit slices. A1, A2 and A3 are the HE staining of Capan-1 tumor, HeLa tumor and the normal skin of BALB/c nude mice forelimb armpit, respectively; B1, B2 and B3 are the Capan-1 tumor slice, HeLa and the normal mice skin slices included with primary antibodies Anti-KRAS antibody (1:150, Catalog Number: 12063-1-AP, Proteintech), respectively. An OLYMPUS VS120 virtual slide microscope was performed the imaging with a 10× objective len.

Tissue Slices Imaging of Probes 1-3. We also evaluated whether probes **1-3** could selectively detect PDEδ protein in the tissue slices. When the tissue slices were antigen repaired, and then incubated with 10 μM probes **1-3** for 12h. The results (**Figure 10**) indicated that Capan-1 tumor slices could be labelled with probe 1-3 and accompany with stronger fluorescence; while the fluorescence intensity of HeLa and normal mice skin tissue slice is relative weaker than Capan-1 tumor slice incubated with probes **1-3**. And the fluorescence intensity of Capan-1 tumor slice incubated with probe and 200 μM deltazinone decreased obviously compared with Capan-1 tumor slice incubated probes **1-3** alone, the results are consist with the cell fluorescence imaging results. The tissue sections imaging results indicated that probes **1-3** could be used into tumor diagnosis in the future.

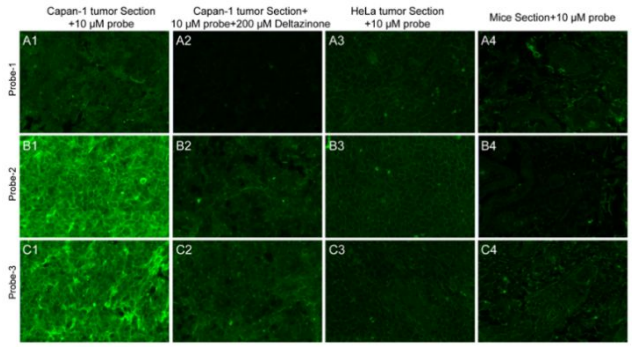

Figure 10. Tissue slices Imagings of probes **1-3**. A1, B1 and C1: Capan-1 tumor + 10 μM probes **1-3**, respectively; A2, B2 and C2: Capan-1 tumor + 10 μM probe **1-3** + 200 μM deltazinone, respectively; A3, B3 and C3: HeLa tumor slices + 10 μM probes **1-3**, respectively; A4, B4 and C4: the normal mice skin slices + 10 μM probes **1-3**, respectively. An OLYMPUS VS120 virtual slide microscope was performed the imaging with a 10× objective len.

CONCLUSION

In the current study, we designed and synthesized three novel small molecule fluorescent probes **1-3** for PDEδ protein, with reasonable fluorescent properties, and high feasibility into detecting and imaging PDEδ protein. After bioactivity evaluation, our probes can be applied into living cell lines and tumor tissues slices imaging, they can down-regulate the mRNA expression of *KRAS*, *PDEδ*, *AKT1*, *MAPK1*, *MEK7*, *RAF1* and *mTOR*, and decrease the protein level of Erk and pErk. Compared with immunofluorescence or fluorescent protein-based techniques, these novel non-peptide small-molecule probes for PDEδ protein are more affordable, rapid, convenient and with turn-on mechanism, and thus resulting in the development of a brand-new type of anticancer candidates. Furthermore, these small-molecule fluorescent probes are hopefully applied into drug screening as well as pathological and physiological studies of the related protein-protein interactions.

ASSOCIATED CONTENT

Supporting Information

More detail of synthetic experiment procedures, NMR and MS spectra. The Supporting Information is available free of charge on the ACS Publications website at DOI: 10.1021/.

AUTHOR INFORMATION

Author Contributions

The final manuscript was approved by all authors.

Conflict of Interest Disclosure

The authors declare no competing financial interest.

ACKNOWLEDGMENT

The project is supported by the National Natural Science Foundation of China (Nos. 21738002 and 81725020), the Shandong Natural Science Foundation (No. ZR2018ZC0233), the Taishan Scholar Program at Shandong Province, the Key Research and Development Project of Shandong Province (No. 2017CXGC1401) and the Innovation Program of Shanghai Municipal Education Commission (No. 2019-01-07-00-07-E00073).

REFERENCES

(1) Polireddy, K.; Chen, Q. Cancer of the Pancreas: Molecular Pathways and Current Advancement in Treatment. *J. Cancer.* **2016**, *7*, 1497-1514.
(2) Grapsa, D.; Saif, M. W.; Syrigos, K. Targeted therapies for pancreatic adenocarcinoma: Where do we stand, how far can we go? *World. J. Gastrointest. Oncol.* **2015**, *7*, 172-177.
(3) Hu, C.; Dadon, T.; Chenna, V.; Yabuuchi, S.; Bannerji, R.; Booher, R.; Strack, P.; Azad, N.; Nelkin, B. D.; Maitra, A. Combined Inhibition of Cyclin-Dependent Kinases (Dinaciclib) and AKT (MK-2206) Blocks Pancreatic Tumor Growth and Metastases in Patient-Derived Xenograft Models. *Mol. Cancer. Ther.* **2015**, *14*, 1532-1539.
(4) Chien, W.; Sun, Q. Y.; Lee, K. L.; Ding, L. W.; Wuensche, P.; Torres-Fernandez, L. A.; Tan, S. Z.; Tokatly, I.; Zaiden, N.; Poellinger, L.; Mori, S.; Yang, H.; Tyner, J. W.; Koeffler, H. P. Activation of protein phosphatase 2A tumor suppressor as potential treatment of pancreatic cancer. *Mol. Oncol.* **2015**, *9*, 889-905.
(5) Eser, S.; Schnieke, A.; Schneider, G.; Saur, D. Oncogenic KRAS signalling in pancreatic cancer. *Br. J. Cancer.* **2014**, *111*, 817-822.
(6) Bryant, K. L.; Mancias, J. D.; Kimmelman, A. C.; Der, C. J. KRAS: feeding pancreatic cancer proliferation. *Trends. Biochem. Sci.* **2014**, *39*, 91-100.
(7) Jiang, Y.; Zhuang, C.; Chen, L.; Lu, J.; Dong, G.; Miao, Z.; Zhang, W.; Li, J.; Sheng, C. Structural Biology-Inspired Discovery of Novel KRAS-PDEdelta Inhibitors. *J. Med. Chem.* **2017**, *60*, 9400-9406.
(8) McCormick, F. K-Ras protein as a drug target. *J. Mol. Med (Berl).* **2016**, *94*, 253-258.
(9) Pang, X.; Liu, M. Defeat mutant KRAS with synthetic lethality. *Small. GTPases.* **2017**, *8*, 212-219.
(10) Ray, D.; Cuneo, K. C.; Rehemtulla, A.; Lawrence, T. S.; Nyati, M. K. Inducing Oncoprotein Degradation to Improve Targeted Cancer Therapy. *Neoplasia.* **2015**, *17*, 697-703.
(11) Rocks, O.; Peyker, A.; Kahms, M.; Verveer, P. J.; Koerner, C.; Lumbierres, M.; Kuhlmann, J.; Waldmann, H.; Wittinghofer, A.; Bastiaens, P. I. An acylation cycle regulates localization and activity of palmitoylated Ras isoforms. *Science.* **2005**, *307*, 1746-1752.
(12) Malumbres, M.; Barbacid, M. RAS oncogenes: the first 30 years. *Nat. Rev. Cancer.* **2003**, *3*, 459-465.
(13) Zorde Khvalevsky, E.; Gabai, R.; Rachmut, I. H.; Horwitz, E.; Brunschwig, Z.; Orbach, A.; Shemi, A.; Golan, T.; Domb, A. J.; Yavin, E.; Giladi, H.; Rivkin, L.; Simerzin, A.; Eliakim, R.; Khalaileh, A.; Hubert, A.; Lahav, M.; Kopelman, Y.; Goldin, E.; Dancour, A.; Hants, Y.; Arbel-Alon, S.; Abramovitch, R.; Shemi, A.; Galun, E. Mutant KRAS is a druggable target for pancreatic cancer. *Proc. Natl. Acad. Sci. U.S.A.* **2013**, *110*, 20723-20728.

(14) Hanahan, D.; Weinberg, R. A. Hallmarks of cancer: the next generation. *Cell.* **2011**, *144*, 646-674.
(15) Warburg, O. On the origin of cancer cells. *Science.* **1956**, *123*, 309-314.
(16) Chandra, A.; Grecco, H. E.; Pisupati, V.; Perera, D.; Cassidy, L.; Skoulidis, F.; Ismail, S. A.; Hedberg, C.; Hanzal-Bayer, M.; Venkitaraman, A. R.; Wittinghofer, A.; Bastiaens, P. I. The GDI-like solubilizing factor PDEdelta sustains the spatial organization and signalling of Ras family proteins. *Nat. Cell. Biol.* **2011**, *14*, 148-158.
(17) Nikolova, S.; Guenther, A.; Savai, R.; Weissmann, N.; Ghofrani, H. A.; Konigshoff, M.; Eickelberg, O.; Klepetko, W.; Voswinckel, R.; Seeger, W.; Grimminger, F.; Schermuly, R. T.; Pullamsetti, S. S. Phosphodiesterase 6 subunits are expressed and altered in idiopathic pulmonary fibrosis. *Respir. Res.* **2010**, *11*, 146.
(18) Zimmermann, G.; Papke, B.; Ismail, S.; Vartak, N.; Chandra, A.; Hoffmann, M.; Hahn, S. A.; Triola, G.; Wittinghofer, A.; Bastiaens, P. I.; Waldmann, H. Small molecule inhibition of the KRAS-PDEdelta interaction impairs oncogenic KRAS signalling. *Nature.* **2013**, *497*, 638-642.
(19) Papke, B.; Murarka, S.; Vogel, H. A.; Martin-Gago, P.; Kovacevic, M.; Truxius, D. C.; Fansa, E. K.; Ismail, S.; Zimmermann, G.; Heinelt, K.; Schultz-Fademrecht, C.; Al Saabi, A.; Baumann, M.; Nussbaumer, P. Identification of pyrazolopyridazinones as PDEdelta inhibitors. *Nat. Commun.* **2016**, *7*, 11360.
(20) Dharmaiah, S.; Bindu, L.; Tran, T. H.; Gillette, W. K.; Frank, P. H.; Ghirlando, R.; Nissley, D. V.; Esposito, D.; McCormick, F.; Stephen, A. G.; Simanshu, D. K. Structural basis of recognition of farnesylated and methylated KRAS4b by PDEdelta. *Proc. Natl. Acad. Sci. U.S.A.* **2016**, *113*, E6766-e6775.
(21) Liu, Z.; Miao, Z.; Li, J.; Fang, K.; Zhuang, C.; Du, L.; Sheng, C.; Li, M. A fluorescent probe for imaging p53-MDM2 protein-protein interaction. *Chem. Biol. Drug. Des.* **2015**, *85*, 411-417.
(22) Liu, T.; Jiang, Y.; Liu, Z.; Li, J.; Fang, K.; Zhuang, C.; Du, L.; Fang, H.; Sheng, C.; Li, M. Environment-sensitive turn-on fluorescent probes for p53–MDM2 protein–protein interaction. *Med.Chem.Comm.* **2017**, *8*, 1668-1672.
(23) Liu, Z.; Jiang, T.; Wang, B.; Ke, B.; Zhou, Y.; Du, L.; Li, M. Environment-Sensitive Fluorescent Probe for the Human Ether-a-go-go-Related Gene Potassium Channel. *Anal. Chem.* **2016**, *88*, 1511-1515.
(24) Liu, J.; Tian, C.; Jiang, T.; Gao, Y.; Zhou, Y.; Li, M.; Du, L. Discovery of the First Environment-Sensitive Fluorescent Probe for GPR120 (FFA4) Imaging. *ACS. Med. Chem. Lett.* **2017**, *8*, 428-432.
(25) Dong, G.; He, S.; Qin, X.; Liu, T.; Jiang, Y.; Li, X.; Chen, L.; Han, G.; Sheng, C.; Li, M. Discovery of Nonpeptide, Environmentally Sensitive Fluorescent Probes for Imaging p53-MDM2 Interactions in Living Cell Lines and Tissue Slice. *Anal. Chem.* **2020**, *92*, 2642-2648.
(26) Lavis, L. D.; Raines, R. T. Bright ideas for chemical biology. *ACS. Chem. Biol.* **2008**, *3*, 142-155.
(27) Chen, L.; Zhuang, C.; Lu, J.; Jiang, Y.; Sheng, C. Discovery of Novel KRAS-PDEdelta Inhibitors by Fragment-Based Drug Design. *J. Med. Chem.* **2018**, *61*, 2604-2610.
(28) Schmittgen, T. D.; Livak, K. J. Analyzing real-time PCR data by the comparative C(T) method. *Nat. Protoc.* **2008**, *3*, 1101-1108.
(29) Zhai, D.; Li, S.; Dong, G.; Zhou, D.; Yang, Y.; Wang, X.; Zhao, Y.; Yang, Y.; Lin, Z. The correlation between DNA methylation and transcriptional expression of human dopamine transporter in cell lines. *Neurosci. Lett.* **2018**, *662*, 91-97.
(30) Downward, J. Targeting RAS signalling pathways in cancer therapy. *Nat. Rev. Cancer.* **2003**, *3*, 11-22.

Table Of Content

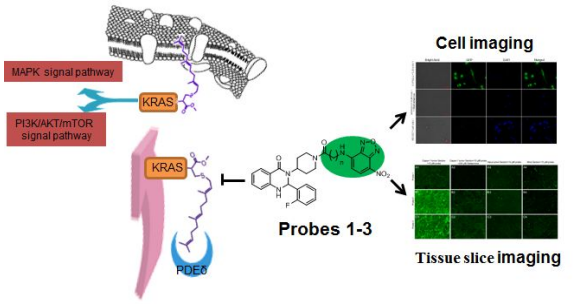
MAPK signal pathway
KRAS
PI3K/AKT/mTOR signal pathway
KRAS
PDE6
Probes 1-3
Cell imaging
Tissue slice imaging